Journal of Histochemistry & Cytochemistry 62(1) 85–96

DOI: 10.1369/0022155413508409
jhc.sagepub.com
SAGE

Peroxiredoxin I and II in Human Eyes: Cellular Distribution and Association with Pterygium and DNA Damage

Sonja Klebe, Thomas Callahan, and John HT Power
Departments of Anatomical Pathology and Human Physiology, School of Medicine, Flinders University, South Australia (SK, TC, JHP)

Summary
Peroxiredoxin I and II are both 2-Cys members of the peroxiredoxin family of antioxidant enzymes and inactivate hydrogen peroxide. On western blotting, both enzymes appeared as 22-kD proteins and were present in the sclera, retina and iris. Immunohistochemistry showed strong cytoplasmic labeling in the basal cells of the corneal epithelial layer and the corneoscleral limbus. The melanocytes within the stroma of the iris and the anterior epithelial cells of the lens also showed strong cytoplasmic labeling. The fibrous structure of the stroma and the posterior surface of the ciliary body were also labeled. There was also strong labeling for both enzymes in the photoreceptors and the inner and outer plexiform layers of the retina. There was increased labeling of peroxiredoxin I and II in pterygium. In normal conjunctiva and cornea, only the basal cell layer showed labeling for peroxiredoxin I and II, whereas, in pterygia, there was strong cytoplasmic labeling in most cells involving the full thickness of the epithelium. Co-localization of the DNA oxidation product 8-hydroxy-2'-deoxyguanosine antibody with the nuclear dye 4',6'-diamidino-2-phenylindole dihydrochloride indicated that the majority of the oxidative damage was cytoplasmic; this suggested that the mitochondrial DNA was most affected by the UV radiation in this condition. (J Histochem Cytochem 62:85–96, 2014)

Keywords
immunohistochemistry, confocal microscopy, 8-hydroxy-2'-deoxyguanosine antibody, western blotting, mitochondria, cornea, iris, lens, retina, ciliary body

Introduction

All mammalian cells use oxygen as a fuel source during mitochondrial respiration and in doing so generate a range of reactive oxygen species (ROS), such as the superoxide radicals and hydrogen peroxide that are damaging to cellular processes. If not inactivated, these ROS lead to oxidative stress with damage to DNA, proteins and lipids. Superoxide dismutase, glutathione peroxidases, catalase and the more recently identified peroxiredoxins inactivate these compounds and thereby protect tissues from oxidative stress.

The eye is particularly vulnerable to oxidative stress, because it lacks the protective keratin layers that are present in skin. In particular, the cornea and conjunctiva are exposed to higher levels of UV-B radiation and higher partial pressures of oxygen than most other tissues. The range of UV-associated eye diseases includes ocular surface squamous neoplasia, cataracts and pterygium, with pterygium having the highest incidence and highest associated health cost in Australia (Shoham et al. 2008; Wlodarczyk et al. 2001). Occasionally, ocular surface squamous neoplasia and invasive squamous cell carcinoma may develop on the basis of a pterygium. Pterygia are reported to have pre-malignant characteristics and are considered to be a potentially pre-cancerous condition, with similarities to the skin

Received for publication April 23, 2013; accepted September 11, 2013.

Corresponding Author:
John H.T. Power, Associate Professor, Department of Human Physiology, School of Medicine, Flinders University, Adelaide, Australia 5042.
Email: john.power@flinders.edu.au

condition solar keratosis, which may progress to squamous cell carcinoma (Weinstein et al. 2002; Chui et al. 2011).

The importance of antioxidant defenses in ocular tissues have been reported in many eye conditions. Increased superoxide dismutase expression has been reported to reduce cone cell death in retinitis pigmentosa and protect the lens from cataract formation (Usui et al. 2009; Lin et al. 2005); although, the absolute expression levels appear to be lower than those in the cornea (Behndig et al. 1998). Similarly, glutathione and catalase are reported to suppress TGFβ-induced cataract-related changes in rat ocular tissues (Chamberlain et al. 2009). Human tear film contains several forms of superoxide dismutase (Crouch et al. 1991; Behndig et al. 1998). There is, however, very little information regarding the distribution of the peroxiredoxin family in ocular tissues and their role in protection against oxidative stress. There are six members of the peroxiredoxin family with peroxiredoxin I-V being the 2-Cys members and peroxiredoxin VI the one 1-Cys member (Wood et al., 2003). Peroxiredoxin I and II have molecular weights of 22.1 kD and 21.8 kD, respectively, and exist as homodimers. They have greater than 80% sequence homology and employ the same mechanism to inactivate hydrogen peroxide. The active site is the redox-active Cys-52, which is oxidized to a Cys-SOH before it further reacts with the Cys-173-SH of the other subunit to form a homodimer. The enzyme may subsequently be regenerated by reduction of the disulfide by thioredoxin. Despite the high degree of homology, it has been recently reported that they are not duplicate proteins and the unique differences impart distinct regulatory roles to each protein in addition to their peroxidase activity (Lee et al. 2007). Peroxiredoxin I knockout leads to uncontrolled cellular proliferation and tumor development, whereas peroxiredoxin II knockout leads to splenomegaly caused by congestion of red pulp with hemosiderin accumulation (Lee et al. 2003; Neumann et al. 2003).

Pterygium is a chronic, wing-shaped proliferative growth of inflamed and vascularized conjunctiva that characteristically encroaches onto the cornea where it may impair vision. A causative role for UV-B radiation is well documented by epidemiological and experimental data; other accepted risk factors include chronic inflammatory processes, alterations in cytokine expression, genetic factors and viruses (Cimpean et al. 2013, Moran and Hollows 1984; Lee et al. 1994; Fox et al. 2013; Siak et al. 2011; Peng et al. 2012; Chalkia et al. 2013). Nonetheless, the underlying molecular mechanisms are poorly understood. The generation of ROS has received some attention recently, and is of particular clinical interest because antioxidant therapies may be a feasible treatment (Tsai et al. 2005; Ucakhan et al. 2009).

Oxidative damage and, more specifically, generation of ROS by UV radiation have been suggested as initiating events in the development of pterygia. ROS can damage cellular DNA with the generation of the oxidized base 8-hydroxy-2'deoxyguanosine (8-OHdG), and its relationship to the tumor suppressor gene p53 has received particular attention (Perra et al. 2006, Cimpean et al. 2013). Further evidence for the importance of ROS in pterygium formation lies in the commonly seen Stocker line, an area of excess iron deposition at the advancing edge of a pterygium. The role of iron in the induction of oxidative stress via the Fenton reaction has been extensively studied in other neoplastic lesions. Many cells and tissues can respond to elevated levels of ROS by increasing the expression and synthesis of protective antioxidant enzymes, such as superoxide dismutase (Usui et al. 2009; Lin et al. 2005), glutathione peroxidase (Power and Blumbergs 2009) and peroxiredoxin VI (Power et al. 2008)

In this work, we have investigated the distribution of the two protective antioxidant enzymes peroxiredoxin I and II in the normal human eye. In addition, we have investigated the distribution of these enzymes in pterygia, where we relate increased expression and cellular protection in response to cellular oxidative DNA damage.

Materials & Methods

Antibodies

Primary antibodies. Peroxiredoxin I and II (rabbit, ab59538, ab59539) were from Abcam (Cambridge, UK). Although there is considerable sequence homology between these two proteins, these two antibodies are made to specific regions of each protein and do not cross react. 8-Hydroxy-2'-deoxyguanosine (8-OHdG) antibody (mouse, ab48508) was also from Abcam.

Secondary antibodies. Goat anti-rabbit alkaline phosphatase (A-3687) was from Sigma Chemical Company (St Louis, MO). Donkey anti-rabbit biotin (711-065-152), donkey anti-rabbit Cy3 (711-165-152), donkey anti-mouse and DyLight 488 (715-485-150) were from Jackson Immunoresearch Laboratories (West Grove, MA). Vector ABC kit was from Vector Laboratories Inc. (Burlingame, CA).

Human Eye Tissue

Institutional ethics approval was obtained for all work presented. Human eye tissues not suitable for transplantation but with consent for research use were obtained from the Flinders Medical Centre Eye Bank. Human eyes were dissected under a dissecting microscope. Sections from pterygium samples were obtained from paraffin blocks of surgical material collected at routine surgical procedures. For immunohistochemical studies, material was fixed in 10% buffered formalin, embedded in paraffin and cut into 6-μm-thick sections. A total of three eyes were obtained for specific tissue extraction for western blotting. Normal eyes

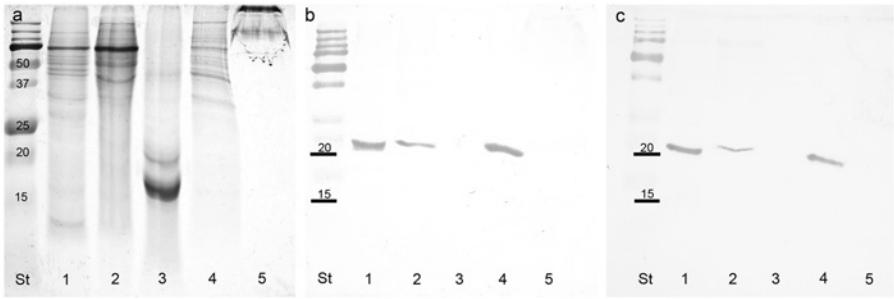

Figure 1. (a,b,c) Coomassie blue-stained PAGE gel of normal human eye tissues (a) and corresponding blots of repeat gels probed with peroxiredoxin I (b) and peroxiredoxin II (c). St, standards in kD; Lane 1, retina; 2, sclera; 3, lens; 4, iris; 5, cornea.

were processed for the immunohistochemical localization of peroxiredoxin I and II, and a total of 12 pterygium samples were investigated and compared with respect to the distribution of peroxiredoxin I and II and co-localization with 8-OHdG.

Western Blotting

Eye tissues were homogenized for 15 sec in homogenizing buffer (50 mM Tris, 5 mM EDTA, 0.1% sodium azide, 1 µl/ml pepstatin and leupeptin and 0.3 mM of phenylmethylsulfonyl fluoride) using a small-tipped Ultra Tarax tissue homogenizer. In addition, cornea and lens tissue was also subjected to 15 sec of ultra-sonication. The homogenates were pelleted a 200 ×g for 10 min and the supernatant was assayed for total protein and snap frozen at -80C.

One-Dimensional Electrophoresis and Western Blotting

Proteins from human eye tissue homogenates were separated using a Bio-Rad Mini-PROTEAN gel system (Bio-Rad, Richmond, CA) on 12% polyacrylamide gels. The separated proteins were transferred onto PVDF membranes using a Semi-Dry Transfer Unit (model TE70 SemiPhor, Hoefer Inc, Holliston, MA) using a transfer buffer of 0.25 M Tris, 0.192 M glycine, and 20% methanol for 90 min at 0.8 mA/cm^2. The PVDF membranes containing the transferred proteins were blocked with milk proteins and incubated overnight at 4C with primary antibodies to peroxiredoxin I and II. The antigen-antibody complex was visualized using a donkey anti-rabbit alkaline phosphatase secondary antibody (Sigma) and BCIP/NBT substrate tablets (Sigma, Cat # B-5655).

Immunohistochemistry

Cellular Localization of Peroxiredoxin I and II. Normal eye sections were deparaffinized, subjected to EDTA antigen retrieval, blocked with 20% normal horse serum and then incubated for 18 hr in a humidified chamber with rabbit antibodies (1/1000) against peroxiredoxin I and II and pre-immune serum. The primary antibodies were visualized with biotinylated goat anti-sheep secondary antibodies (Sigma) and the antibody complex visualized using a Vector ABC kit and Vector Red (SK-5100) substrate. Sections were examined and photographed with an Olympus BX50 microscope using a 100× objective with oil immersion linked to a QImaging Micro Publisher 5.0 RTV camera (Olympus, Canada). A montage of these images taken at 100 × magnification was then assembled in Adobe Photoshop (Adobe Systems Inc., San Jose, CA).

In the pterygium sections, peroxiredoxin I and II were each co-localized with antibodies to 8-OHdG, and the nuclear dye 4',6'-diamidino-2-phenylindole dihydrochloride (DAPI) (cat # 32670, Sigma). The primary antibodies were visualized using donkey anti-rabbit (Cy3) and donkey anti-mouse (DyLight 488) secondary antibodies (Jackson Immunoresearch Laboratories). Sections were examined using a Leica TCS SP5 Confocal microscope (Leica Microsystems, Wetzlar, Germany).

Results

Characterization of the Peroxiredoxin I and II Antibody in Human Eye Tissue

Human eye proteins (10 µg per well) from various control eye tissues were separated using PAGE and stained with Coomassie blue, as shown in Figure 1a. Sclera and retina had a similar protein profile but the retina had an abundant protein at approximately 10 kD. The iris had a similar protein profile to the sclera but a different distribution in terms of amounts. The lens tissue consisted predominately of two proteins of 20 and 16 kD molecular weight, which ran as broad, heavily staining bands. Although the corneal protein sample was the same concentration as other samples, the proteins were of a higher molecular weight and only migrated a short distance into the gel.

On western blots, both peroxiredoxin I and II were clearly visible as strongly staining bands at approximately 22 kD for samples from the retina and iris, with a lesser band detected in sclera tissue samples (Figs. 1b and 1c). Neither peroxiredoxin I nor peroxiredoxin II were detected on western blots of lens or corneal tissue. When gels and blots were loaded with 20 μg per well, the gels were distorted but the western blots showed the same staining profile. Dot blots using each antibody against both antigens indicated that both antibodies were specific for their respective antigens.

Cellular Distribution of Peroxiredoxin I and II in Human Eye Tissues

Cornea, Conjunctiva and Lens. Peroxiredoxin I and II both showed cytoplasmic labeling of the basal cells of the corneal epithelial layer (Figs. 2a, 2b). This labeling was not uniform and the staining was more prominent toward the corneoscleral junction. The central region of the cornea did not appear to have any labeling. No labeling was present in the underlying acellular Bowman's layer or the collagenous stroma but some nuclei of the keratocytes within the stroma showed positive labeling for peroxiredoxin I. There was also cytoplasmic labeling of the corneal endothelial cells for both peroxiredoxin I and II, again with no staining of the nucleus (Figs. 2d, 2e). The basal cells of the corneoscleral limbus showed prominent cytoplasmic labeling for peroxiredoxin I and II, but no staining in the nucleus (Figs. 2g, 2h). The connective tissue within the conjunctiva showed strong specific cellular labeling for peroxiredoxin I but not for peroxiredoxin II (Figs. 2j, 2k). The anterior lens epithelial cells showed strong cytoplasmic and membrane labeling for both peroxiredoxin I and II but the lens tissue itself was negative (Figs. 2m, 2n). The remaining tissues were negative. The negative control tissue using pre-immune serum did not show any labeling for peroxiredoxin I or II (Figs. 2c, 2f, 2i, 2l, 2o).

Iris and Ciliary Body. Some labeling was present within the melanocytes of the iris but the pigments within the melanocytes of the posterior leaflet made it difficult to determine the extent of peroxiredoxin staining. Peroxiredoxin I showed more prominent staining of cells with a fibrous structure within the stroma of the iris than peroxiredoxin II (Figs. 3a, 3b). The epithelium of the anterior surface of the iris also showed staining for both peroxiredoxin I and II, which was well above the background pigment staining within the control tissue (Figs. 3d, 3e). The negative control tissue using pre-immune serum did not show any labeling for peroxiredoxin I or II within the iris (Figs. 3, 3c, 3f).

There was extensive staining of peroxiredoxin I and II within the fibrous structure of the stroma of the ciliary body (Figs. 3g, 3h). Specific cells within the epithelium of the anterior surface of the ciliary body pars plicata showed staining for both peroxiredoxin I and II (Figs. 3j, 3k). This staining became more intense just prior to the junction with the retina at the pars plana. Cells within the epithelium were positive for peroxiredoxin I and II and clusters of cells just beneath the epithelium with a glandular structure were also positive for peroxiredoxin I and II (Figs. 3m, 3n). The negative control tissue using pre-immune serum did not show any labeling for peroxiredoxin I or II within the ciliary body and the surrounding structures (Figs. 3i, 3l, 3o).

Choroid and Retina. Figure 4 is a montage of high-powered images of immunohistochemical staining for peroxiredoxin I and II that was assembled in Adobe Photoshop to reconstruct the three regions of the retina: a) the choroid; b) the rods and cones, the outer nuclear layer and the outer plexiform layers; and c) the inner nuclear layer, the inner plexiform layer and the nerve fiber layer. Specific cells within the choroid were strongly positive for peroxiredoxin I and weakly positive for peroxiredoxin II. Cells within the pigmented layer of the choroid were also positive for both peroxiredoxin I and II. Both rods and cones were positive for peroxiredoxin I and II, with the cones staining more intensely. Specific nuclei within the photoreceptor layer were positive for both peroxiredoxin I and II. Fibers within the outer plexiform layer were positive for both peroxiredoxin 1 and II but more intensely stained for peroxiredoxin II. Specific nuclei within the inner nuclear layer were strongly positive for peroxiredoxin II and weakly positive for peroxiredoxin I. Fibers within the inner plexiform layer were more positive for peroxiredoxin II than peroxiredoxin I. The nuclei within the ganglion cell layer were not positive for peroxiredoxin I or II. The negative control tissue using pre-immune serum did not show any labeling for peroxiredoxin I or II within the choroid and retina (Fig. 4c).

Distribution of Peroxiredoxin I and II in Pterygium

In pterygium samples, there was strong staining for peroxiredoxin I and II. Whereas normal conjunctiva and cornea showed cytoplasmic labeling of the basal cell layer, pterygium sections showed strong membranous and cytoplasmic labeling in most cells that involved the whole thickness of the epithelium (Figs. 5, 6). Figure 6 shows two additional cases of pterygium at higher magnification. It is clear from 8-OHdG and DAPI labeling that there is very little nuclear labeling. Interestingly, DNA intracellular damage (seen as green dot-like labeling in Figs. 5c, 5d and 6f) is predominantly present in the cytoplasm of the epithelial cells, in some cells in a perinuclear distribution, but with relatively few nuclear signals (white arrow in Fig. 6d); this suggests

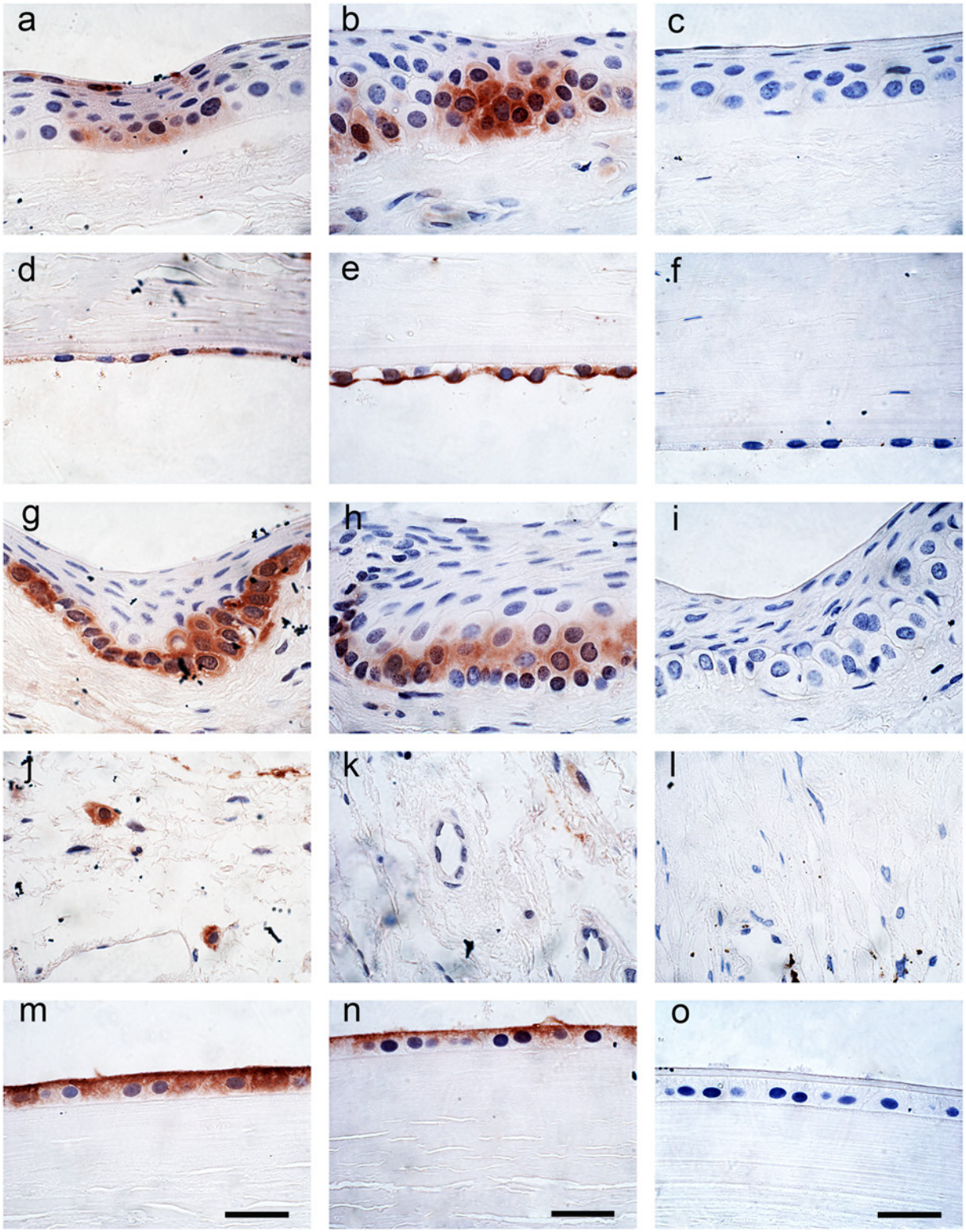

Figure 2. Immunohistochemical localization of peroxiredoxin I (1/1000) (left panel) and peroxiredoxin II (1/1000) (center panel) and pre-immune serum (right panel) in cornea and lens epithelium. (a,b,c) cornea epithelium; (d,e,f) cornea endothelium; (g,h,i) conjunctiva; (j,k,l) conjunctiva connective tissue; and (m,n,o) lens epithelium. All panels are at the same magnification. Scale bars = 10 μm.

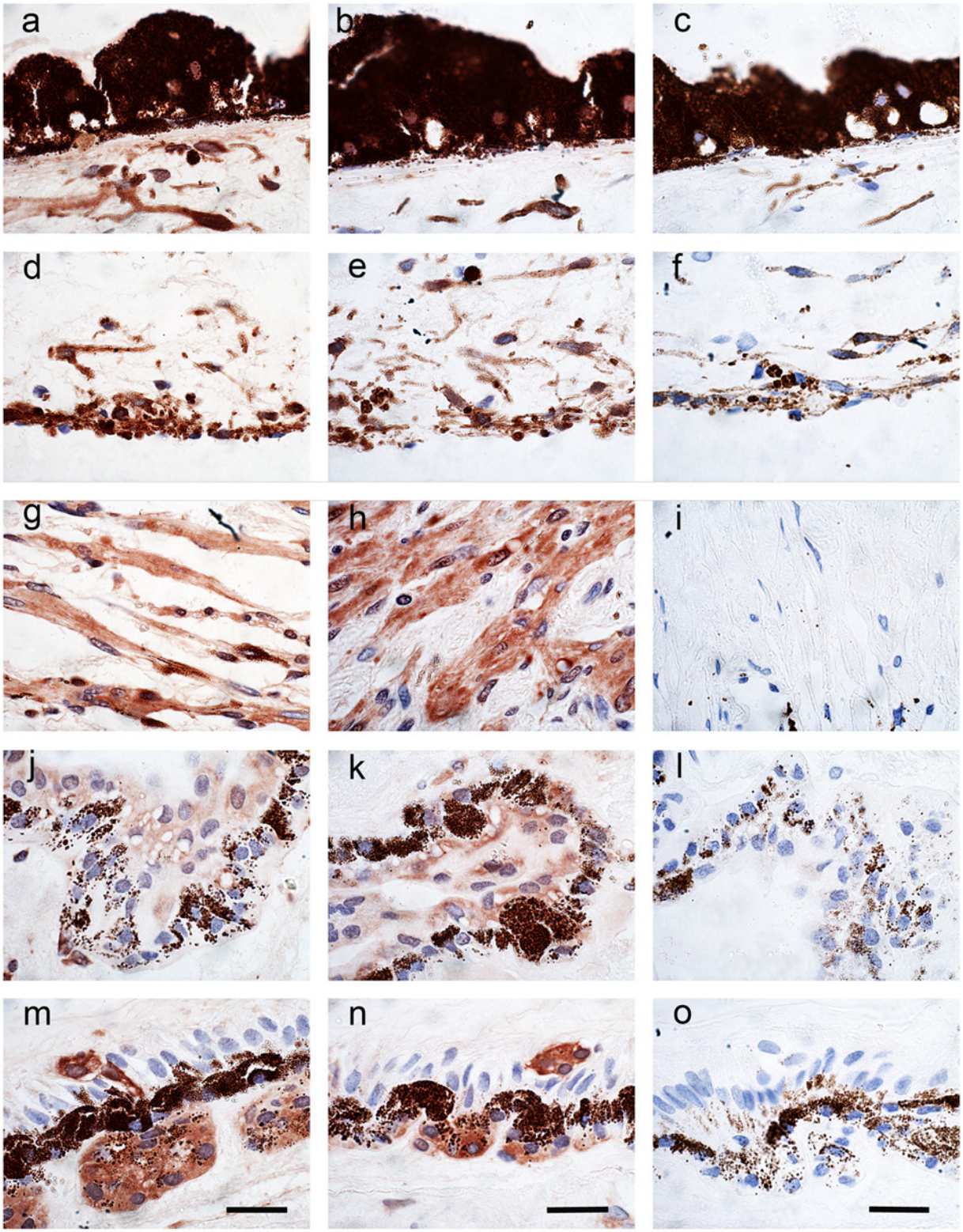

Figure 3. Immunohistochemical localization of peroxiredoxin I (1/1000) (left panel) and peroxiredoxin II (1/1000) (center panel) and pre-immune serum (right panel) in the iris and ciliary body. (a,b,c) iris (internal surface); (d,e,f) iris (external surface); (g,h,i) ciliary body connective tissue; (j,k,l) ciliary body internal surface; and (m,n,o) ciliary body pars plana anterior surface. All panels are at the same magnification. Scale bars = 10 μm.

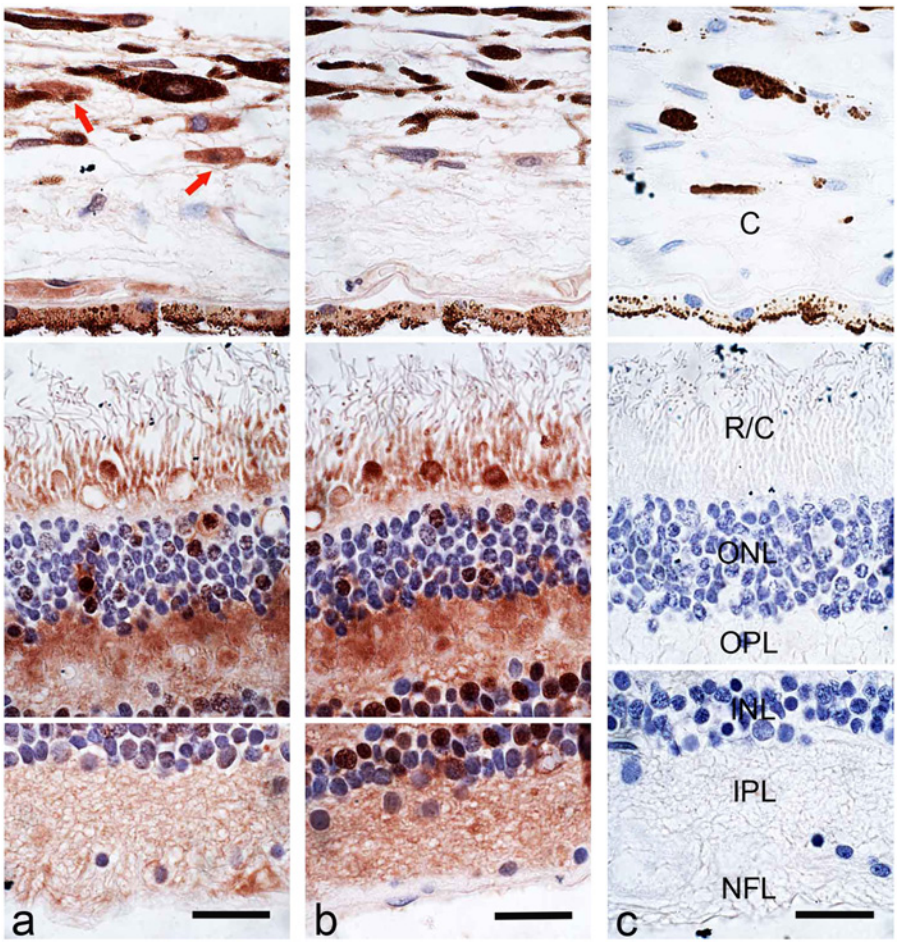

Figure 4. A composite of the immunohistochemical localization of peroxiredoxin I (1/1000) (a), peroxiredoxin II (1/1000) (b) and pre-immune serum (1/1000) (c) in the retina and choroid. Red arrows indicate peroxiredoxin I-positive cells in the choroid. Labels: (C) choroid, (R/C) rods and cones, (ONL) outer nuclear layer, (OPL) outer plexiform layer, (INL) inner nuclear layer, (IPL) inner plexiform layer, (NFL) nerve fiber layer. All panels are at the same magnification. Scale bars = 10μm.

that the majority of UV damage may have been to mitochondrial DNA, rather than nuclear DNA. The greatest level of 8-OHdG damage was present in the surface component of the epithelium (white arrows in Figs. 6e, 6f). This is in keeping with the hypothesis of solar damage, as the surface epithelial cells would have been affected by the highest degree of UV radiation.

Discussion

This is the first paper to systematically describe the distribution of peroxiredoxin I and II in normal and diseased human eyes tissues, and to co-localize expression with a histological marker of oxidative-type DNA damage in a UV-B–associated disorder. Not surprisingly, there was expression of peroxiredoxin I and II in all tissues that were exposed to sunlight, namely the cornea, conjunctiva, lens and retina.

The peroxiredoxin I and II antibodies used in this study were created against specific regions of each protein and did not cross react. Western blots using human eye tissue showed that peroxiredoxin I and II are both present in sclera, retina and iris but most abundantly in the retina and iris. We did not detect either antigen in the lens or corneal tissues using western blotting but did detect positive expresion in the lens epithelial cells and corneal epithelial cells at the corneoscleral limbus using immunohistochemistry. Lens and corneal tissue were difficult to homogenize, and thus both required mechanical homogenization and ultrasonication. Both tissues are largely acellular. The lens has a high protein content comprising fibers of water-soluble crystalline proteins of around 16–20 kD when prepared in reducing sample buffer with SDS. Because the lens extracts had such a large protein concentration and the epithelial cell protein comprised such a low proportion of the total protein, the amount of peroxiredoxin I and II present in these

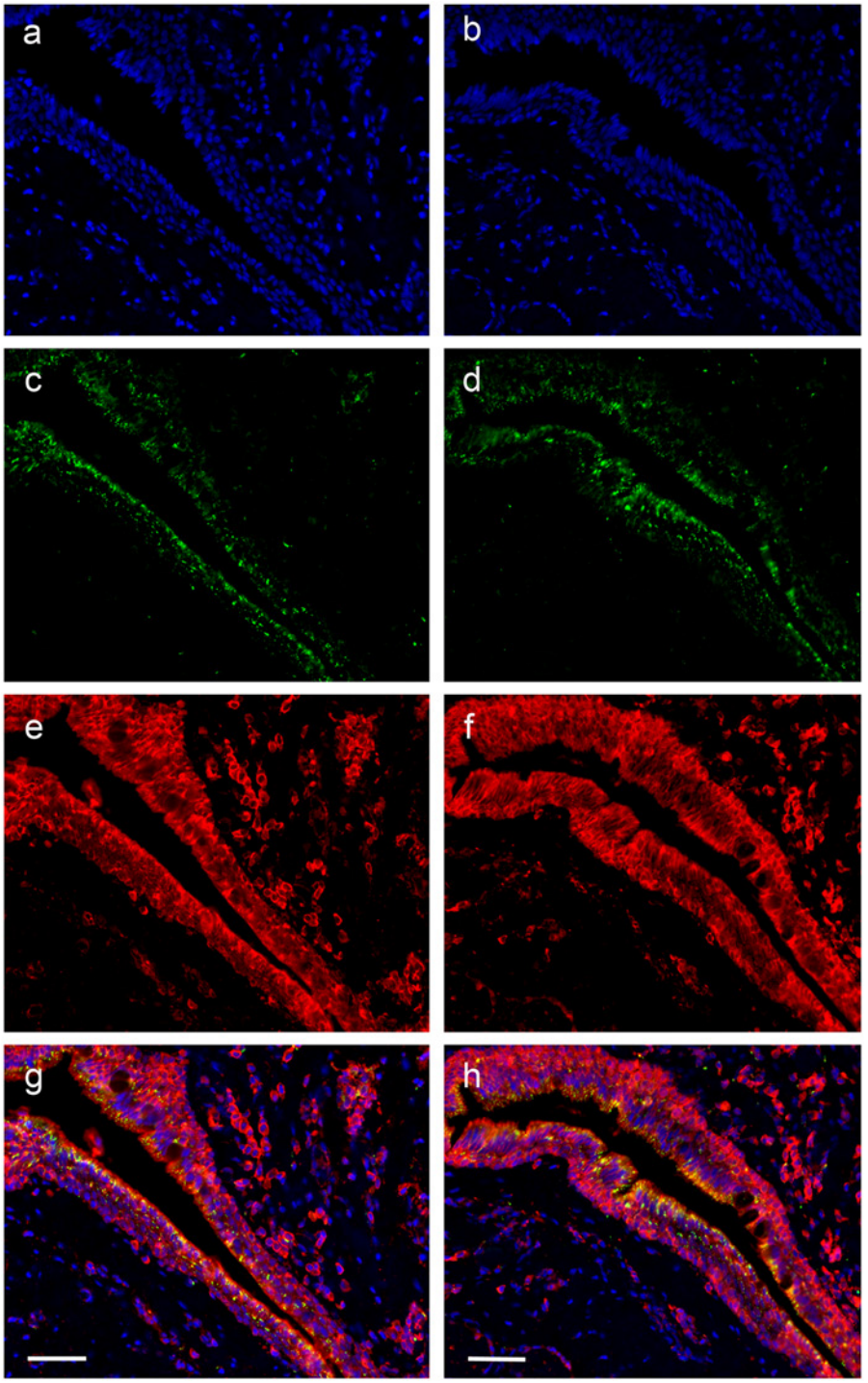

Figure 5. Low-power immunohistochemical localization of the nuclear dye DAPI (blue) (a,b); DNA oxidation product 8-OHdG (DyLight 488-green) (c, d); peroxiredoxin I (1/200) (Cy3-red) (e); peroxiredoxin II (1/200) (Cy3-red) (f); and the merged images (g, h) for one case of pterygium. Scale bars = 30 µm.

samples was likely below the limit of detection on our western blots. The corneal stroma comprises mainly type 1 collagen, which is resistant to reducing agents and is estimated to be 1000 kD when separated using PAGE (Wollensak and Redl 2008). We observed the same PAGE results with a large protein band that only just entered the gel and was not positive for peroxiredoxin I and II on western blots. A second reason for the lack of detection was that some of the

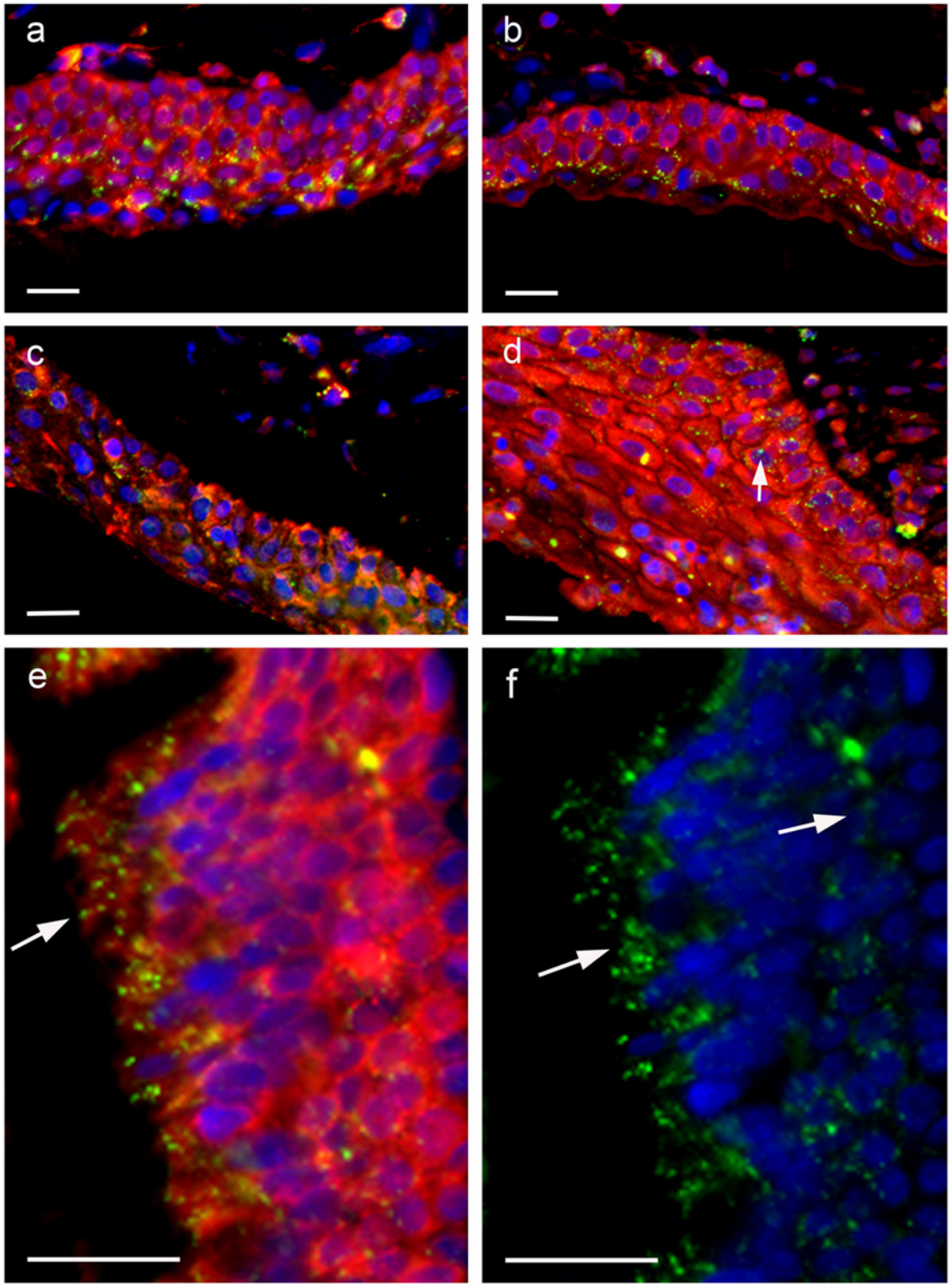

Figure 6. Immunohistochemical localization of peroxiredoxin I (1/200, Cy3-red) and peroxiredoxin II (1/200, Cy3-red) in four different cases of pterygium. Two cases were stained with peroxiredoxin I (a, c) and two cases were stained with peroxiredoxin II (b, d). Nuclei are stained with the nuclear dye DAPI (blue) and DNA oxidation with the 8-OHdG antibody (DyLight 488-green). Arrow in d indicates nuclear staining. (e) High-power image of a pterygium stained with peroxiredoxin I (Cy3-red) and 8-OHdG (DyLight 488-green). Arrow indicate 8-OHdG staining. (f) High-power image of pterygium stained with DAPI (blue) and 8-OHdG (DyLight 488-green). Arrows indicate 8-OHdG staining. Scale bars = 10 μm.

cornea remained attached to the sclera during dissection so as not to contaminate the corneal tissue with sclera, which is known to be positive for peroxiredoxin I and II. Peroxiredoxin I and II were most abundant at the corneoscleral junction and this was the tissue that was left attached to the sclera after corneal dissection. An identical blot was also probed with an actin antibody as a loading control. Actin is a cellular microfilament protein and produced similar results for retina, sclera and iris; however, because the lens and cornea are largely acellular, these samples were negative (result not shown). Apart from the lens and corneal tissues, the results from immunohistochemical labeling in the eye tissue mirrored that of western blotting.

Immunohistochemical labeling of control tissues indicated that peroxiredoxin I and II had predominately a cytoplasmic distribution, although the corneal epithelial cells showed some nuclear labeling. These tissues were stained using the Vector-red substrate, as this produced the best contrast with the pigment in the eye tissues. These control sections were also stained using immunofluorescence and with the DAB substrate. The pigment had marked autofluorescence, particularly in the iris, which made it difficult to distinguish specific labeling. Similarly, the brown staining of the DAB substrate was very similar to the pigment.

Both peroxiredoxins are reported to be cytoplasmic; yet, in eye tissues, variable subcellular distribution levels were observed that may suggest that these enzymes serve different purposes in different tissues. Peroxiredoxin I and II both inactivate hydrogen peroxide and appeared to be upregulated in pterygium, which would imply that hydrogen peroxide levels are elevated in this disorder. UV-B radiation has been associated with pterygium formation and there is considerable data indicating that UV-B radiation can lead to ROS formation. It is hard to be definitive on this point, as the peroxiredoxin I and II in pterygium tissue was imaged using confocal immunofluorescence but the normal eye tissue was examined using light immunohistochemistry and Vector red staining. What this result does support, however, is that the pterygium tissue is an outgrowth from the basal cells of the corneoscleral limbus, which had pockets of cells also strongly positive for peroxiredoxin I and II. For ethical reasons, we could not obtain fresh pterygium tissue to measure protein expression, as this had to be used for pathological assessments. Recent evidence in mouse keratinocytes has indicated that this staining pattern is associated with the increased expression of antioxidant enzymes, which is consistent with our observations (Black 2008). There is mounting evidence that oxidative damage plays a role in a number of degenerative ocular conditions, including Fuchs' endothelial dystrophy (Jurkunas et al. 2008; Wang et al. 2007). In the cornea, a role for peroxiredoxin VI has previously been demonstrated in wound healing (Pak et al. 2006; Tchah et al. 2005). In the human intraocular lens, the expression of peroxiredoxin III and VI has previously been shown in lens epithelium and stroma, and an increase in expression levels in cataract specimens has been well established, suggesting a role for these enzymes in protection from oxidative stress (Hasanova et al. 2009; Kubo et al. 2008; Moreira et al. 2008).

In the iris, we found nuclear expression of peroxiredoxin I and II. This has not been previously reported, but alterations to peroxiredoxin II expression due to promoter methylation have been reported in dermal malignant melanomas. Interestingly, peroxiredoxin II expression in these samples was cytoplasmic, rather than nuclear, as seen in the iris (Furuta et al. 2006). Expression of peroxiredoxin VI has been shown to be involved in homeostasis of metabolic processes in the retina (Zamora et al. 2007; Fatma et al. 2008). Peroxiredoxin III, which is expressed within mitochondria, has been found in cones of the primate retina, where it is thought to contribute to the protection of photoreceptor mitochondria.

In normal tissues, the expression of peroxiredoxin I and II was highest in the mitotically active basal cell layer, possibly indicating a protective role for these enzymes for the most vulnerable, least differentiated and biologically most valuable cells in the cornea and conjunctiva. This zonation pattern was lost in pterygia, where both peroxiredoxins were expressed throughout the entire thickness of the epithelial layer; this suggests that expression had been induced along with cellular proliferation. This profile was associated with cytoplasmic accumulation of DNA damage as detected by the 8-OHdG antibody in the cytoplasm, which may represent mitochondrial DNA damage (Kau et al. 2006; Maxia et al. 2008). A similar DNA damage profile has been reported in the substantia nigra in Parkinson's disease using an 8-OHdG antibody; this was also attributed to mitochondrial DNA damage (Zhang et al. 1999). Interestingly, very little nuclear damage was observed in the pterygium samples. All pterygium samples used in this study comprised several cell layers that were positive for peroxiredoxin I and II, but the major DNA damage was confined to the epithelial cell layers, reinforcing the concept of UV damage. This data suggests that UV-induced tissue damage may promote cellular proliferation and also upregulate the expression of peroxiredoxin I and II in these diseased tissues. This concept is supported by a recent study showing the presence of thymine dimers in the epithelial and stromal components in pterygium, which is related to UV inactivation of the protective p53 gene (Cimpean et al. 2013).

In summary, we have localized the expression of peroxiredoxin I and II to various compartments of the human eye, and demonstrated alterations in their expression patterns in a pathological UV-B–associated processes. The surface of the eye is highly accessible to topical treatment, and future study directions could include topical antioxidant therapy as a first-line treatment for low-grade ocular surface disorders.

Acknowledgments

We acknowledge the support and assistance of the Flinders Medical Centre Eye Bank in obtaining the eye tissues for this project and the excellent assistance of the Flinders University Microscopy and Image Analysis Facility. We also acknowledge the excellent technical assistance of Ms Olivia Barnes and Negara Tajbakhsh.

Declaration of Conflicting Interests

The author(s) declared no potential conflicts of interest with respect to the research, authorship, and/or publication of this article.

Funding

The author(s) disclosed receipt of the following financial support for the research, authorship, and/or publication of this article: Thomas Callahan was supported by a medical school scholarship provided by the Royal College of Pathologists of Australia.

References

Behndig A, Svensson B, Marklund S, Karlsson K (1998). Superoxide dismutase isoenzymes in the human eye. Invest Ophthalmol Vis Sci 39:471-475.

Black AT, Gray JP, Shakarjian MP, Laskin DL, Heck DE, Laskin JD (2008). Distinct effects of ultraviolet B light on antioxidant expression in undifferentiated and differentiated mouse keratinocytes. Carcinogenesis 29:219-225.

Chalkia AK, Spandidos DA, Detorakis ET (2013). Viral involvement in the pathogenesis and clinical features of ophthalmic pterygium (Review). Int J Mol Med 32:539-543.

Cimpean AM, Sava MP, Raica M (2013). DNA damage in human pterygium: One-shot multiple targets Mol Vis 19: 348–356.

Chamberlain CG, Mansfield KJ, Cerra A (2009). Glutathione and catalase suppress TGFbeta-induced cataract-related changes in cultured rat lenses and lens epithelial explants. Mol Vis 15:895-905.

Chui J, Coroneo MT, Tat LT, Crouch R, Wakefield D, Di Girolamo N (2011). Ophthalmic pterygium: a stem cell disorder with premalignant features. Am J Pathol 178:817-827.

Crouch RK, Goletz P, Snyder A, Coles WH (1991). Antioxidant enzymes in human tears. J Ocul Pharmacol 7:253-258.

Fatma N, Kubo E, Sen M, Agarwal N, Thoreson WB, Camras CB, Singh DP (2008). Peroxiredoxin 6 delivery attenuates TNF-alpha-and glutamate-induced retinal ganglion cell death by limiting ROS levels and maintaining Ca^{2+} homeostasis. Brain Res 1233:63-78.

Fox T, Gotlinger KH, Dunn MW, Lee OL, Milman T, Zaidman G, Schwartzman ML, Bellner L (2013). Dysregulated heme oxygenase-ferritin system in pterygium pathogenesis. Cornea 32:1276-1282.

Furuta J, Nobeyama Y, Umebayashi Y, Otsuka F, Kikuchi K, Ushijima T (2006). Silencing of Peroxiredoxin 2 and aberrant methylation of 33 CpG islands in putative promoter regions in human malignant melanomas. Cancer Res 66:6080-6086.

Hasanova N, Kubo E, Kumamoto Y, Takamura Y, Akagi Y (2009). Age-related cataracts and Prdx6: correlation between severity of lens opacity, age and the level of Prdx 6 expression. Br J Ophthalmol 93:1081-1084.

Jurkunas UV, Rawe I, Bitar MS, Zhu C, Harris DL, Colby K, Joyce NC (2008). Decreased expression of peroxiredoxins in Fuchs' endothelial dystrophy. Invest Ophthalmol Vis Sci 49:2956-2963.

Kau HC, Tsai CC, Lee CF, Kao SC, Hsu WM, Liu JH, Wei YH (2006). Increased oxidative DNA damage, 8-hydroxydeoxyguanosine, in human pterygium. Eye 20:826-831.

Kubo E, Fatma N, Akagi Y, Beier DR, Singh SP, Singh DP (2008). TAT-mediated PRDX6 protein transduction protects against eye lens epithelial cell death and delays lens opacity. Am J Physiol 294:C842-C855.

Lee GA, Hirst LW, Sheehan M (1994). Knowledge of sunlight effects on the eyes and protective behaviours in the general community. Ophthalmic Epidemiol 1:67-84.

Lee TH, Kim SU, Yu SL, Kim SH, Park DS, Moon HB, Dho SH, Kwon KS, Kwon HJ, Han YH, Jeong S, Kang SW, Shin HS, Lee KK, Rhee SG, Yu DY (2003). Peroxiredoxin II is essential for sustaining life span of erythrocytes in mice. Blood 101:5033-5038.

Lee W, Choi KS, Riddell J, Ip C, Ghosh D, Park JH, Park YM (2007). Human peroxiredoxin 1 and 2 are not duplicate proteins: the unique presence of CYS83 in Prx1 underscores the structural and functional differences between Prx1 and Prx2. J Biol Chem 282:22011-22022.

Lin D, Barnett M, Grauer L, Robben J, Jewell A, Takemoto L, Takemoto DJ (2005). Expression of superoxide dismutase in whole lens prevents cataract formation. Mol Vis 11:853-858.

Maxia C, Perra MT, Demurtas P, Minerba L, Murtas D, Piras F, Corbu A, Gotuzzo DC, Cabrera RG, Ribatti D, Sirigu P (2008). Expression of survivin in pterygium and relationship with oxidative DNA damage. J Cell Mol Med 12:2372-2380.

Moran DJ, Hollows FC (1984). Pterygium and ultraviolet radiation: a positive correlation. Br J Ophthalmol 68:343-346.

Moreira EF, Kantorow M, Rodriguez IR (2008). Peroxiredoxin 3 (PDRX3) is highly expressed in the primate retina especially in blue cones. Exp Eye Res 86:452-455.

Neumann CA, Krause DS, Carman CV, Das S, Dubey DP, Abraham JL, Bronson RT, Fujiwara Y, Orkin SH, Van Etten RA (2003). "Essential role for the peroxiredoxin Prdx1 in erythrocyte antioxidant defence and tumour suppression". Nature 424: 561–565.

Pak JH, Choi HJ, Choi CY, Tchah H (2006). Expression of 1-cys peroxiredoxin in the corneal wound-healing process. Cornea 25:S29-S35.

Peng ML, Tsai YY, Chiang CC, Huang YC, Chou MC, Yeh KT, Lee H, Cheng YW (2012). CYP1A1 protein activity is associated with allelic variation in pterygium tissues and cells. Mol Vis 18:1937-1943.

Perra MT, Maxia C, Corbu A, Minerba L, Demurtas P, Colombari R, Murtas D, Bravo S, Piras F, Sirigu P (2006). Oxidative stress in pterygium: relationship between p53 and 8-hydroxydeoxyguanosine. Mol Vis 12:1136-1142.

Power JHT, Asad S, Chataway T, Chegini F, Manavis J, Temlett JA, Jensen PH, Blumbergs PC, Gai W (2008). Peroxiredoxin 6 in human brain: molecular forms, cellular distribution and associations with Alzheimer's disease pathology. Acta Neuropath 115:611-622.

Power JHT, Blumbergs PC (2009). Cellular glutathione peroxidase in human brain: cellular distribution, and its potential

role in the degradation of Lewy bodies in Parkinson's disease and dementia with Lewy bodies. Acta Neuropath 117:63-73.

Shoham A, Hadziahmetovic M, Dunaief JL, Mydlarski MB, Schipper HM (2008). Oxidative stress in diseases of the human cornea. Free Radic Biol Med 45:1047-1055.

Siak JJ, Ng SL, Seet LF, Beuerman RW, Tong L (2011). The nuclear-factor kappaB pathway is activated in pterygium. Invest Ophthalmol Vis Sci 52:230-236.

Tchah H, Kim MJ, Kim TI, Choi HJ, Kim JY, Kim MJ, Pak JH (2005). Regulation of 1-cys peroxiredoxin expression in the process of stromal wound healing after photorefractive keratectomy. Invest Ophthalmol Vis Sci 46:2396-2403.

Tsai YY, Cheng YW, Lee H, Tsai FJ, Tseng SH, Lin CL, Chang KC (2005). Oxidative DNA damage in pterygium. Mol Vis 11:71-75.

Ucakhan OO, Kanpolat A, Elgun S, Durak I (2009). The role of oxidative mechanisms in the etiopathogenesis of pterygium: a preliminary study. Opthalmologica 223:41-46.

Usui S, Oveson BC, Lee SY, Jo YJ, Yoshida T, Miki A, Miki K, Iwase T, Lu L, Campochiaro PA. (2009). NADPH oxidase plays a central role in cone cell death in retinitis pigmentosa. J Neurochem 110:1028-1037.

Wang Z, Handa JT, Green WR, Stark WJ, Weinberg RS, Jun AS (2007). Advanced glycation end products and receptors in Fuchs' dystrophy corneas undergoing Descemet's stripping with endothelial keratoplasty. Ophthalmology 114:1453-1460.

Weinstein O, Rosenthal G, Zirkin H, Monos T, Lifshitz, Argov S (2002). Overexpression of p53 suppressor gene in pterygia. Eye 16:619-621.

Wlodarczyk J, Whyte P, Cockrum P, Taylor H (2001). Pterygium in Australia: a cost of illness study. Clin Exp Ophthalmol 29:370-375.

Wollensak G, Redl B (2008). Gel electrophoretic analysis of corneal collagen after photodynamic cross-linking treatment. Cornea 27:353-356

Wood ZA, Schroder E, Harris JR (2003). Poole LB Structure, mechanism and regulation of peroxiredoxins. Trend Biochem Sci 28:32-40.

Zamora DO, Riviere M, Choi D, Pan Y, Planck SR, Rosenbaum JT, David LL, Smith JR (2007). Proteomic profiling of human retinal and choroidal endothelial cells reveals molecular heterogeneity related to tissue of origin. Mol Vis 13: 2058-2065.

Zhang J, Perry G, Smith MA, Robertson D, Olson SJ, Graham DG, Montine TJ (1999). Parkinson's disease is associated with oxidative damage to cytoplasmic DNA and RNA in substantia nigra neurons. Am J Path 154:1423-1429.